Biophysics of Cadherin Adhesion

ARTICLE *in* SUB-CELLULAR BIOCHEMISTRY · JUNE 2012

DOI: 10.1007/978-94-007-4186-7_4 · Source: PubMed

2 AUTHORS:

Deborah E Leckband
University of Illinois, Urbana…

162 PUBLICATIONS **7,217** CITATIONS

SEE PROFILE

Sanjeevi Sivasankar
Iowa State University

36 PUBLICATIONS **790** CITATIONS

SEE PROFILE

Chapter 4
Biophysics of Cadherin Adhesion

Deborah Leckband and Sanjeevi Sivasankar

Abstract Since the identification of cadherins and the publication of the first crystal structures, the mechanism of cadherin adhesion, and the underlying structural basis have been studied with a number of different experimental techniques, different classical cadherin subtypes, and cadherin fragments. Earlier studies based on biophysical measurements and structure determinations resulted in seemingly contradictory findings regarding cadherin adhesion. However, recent experimental data increasingly reveal parallels between structures, solution binding data, and adhesion-based biophysical measurements that are beginning to both reconcile apparent differences and generate a more comprehensive model of cadherin-mediated cell adhesion. This chapter summarizes the functional, structural, and biophysical findings relevant to cadherin junction assembly and adhesion. We emphasize emerging parallels between findings obtained with different experimental approaches. Although none of the current models accounts for all of the available experimental and structural data, this chapter discusses possible origins of apparent discrepancies, highlights remaining gaps in current knowledge, and proposes challenges for further study.

4.1 Introduction

The assembly and maintenance of intercellular junctions is central to the role of cadherins in morphogenesis and disease. A challenge is to determine how classical cadherins assemble junctions, and how sequence differences, mutations, and post-translational modifications alter this function. Classical cadherins are transmembrane proteins. The extracellular segment, which embeds the adhesive function, folds into five extracellular (EC) domains, numbered 1–5 from the N-terminal domain (EC1-5) (Fig. 4.1a).

D. Leckband (✉)
Department of Chemistry, Department of Chemical and Biomolecular Engineering, Center for Biophysics and Computational Biology, University of Illinois at Urbana-Champaign, 600 South Mathews Ave, Urbana, IL, 61801, USA
e-mail: leckband@illinois.edu

S. Sivasankar
Department of Physics and Astronomy, Iowa State University, A319 Zaffarano Hall, Aimes, IA 50011, USA
e-mail: sivsank@iastate.edu

T. Harris (ed.), *Adherens Junctions: From Molecular Mechanisms to Tissue Development and Disease,* Subcellular Biochemistry 60,
DOI 10.1007/978-94-007-4186-7_4,

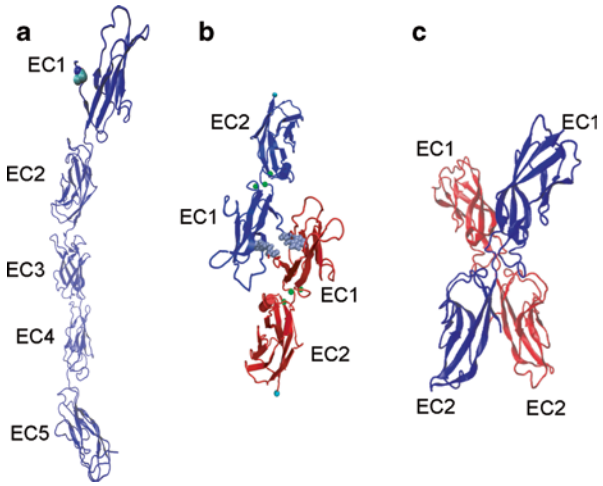

Fig. 4.1 Cadherin structures. **a** Crystal structure of the extracellular region of *Xenopus* C-Cadherin showing the W2 residue (cyan van der Waals structure) (Boggon and Eck 2004). **b** Strand-swapped dimer between E-cadherin EC1-2 fragments. Here the W2 residues (gray van der Waals structures) bridge the apposing EC1 domains, and the calcium ions are shown as green Van der Waals structures. **c** X-dimer of the W2A mutant of E-cadherin EC1-2 fragments. The adjacent domains form a tetrahedral structure with extensive contacts at the inter-domain junction. (Harrison et al. 2010)

The several approaches used to investigate the mechanism of cadherin binding probe different aspects of cadherin function. Structure determinations contributed to our present understanding of binding interfaces and global protein organization at inter-membrane junctions. Static images do not, however, reveal crucial biophysical properties such as kinetic rates, affinities, and adhesion energies that determine the assembly dynamics and mechanical integrity of intercellular junctions. Thus, solution binding and mechanical measurements generate complementary mechanistic insights into cadherin functions, but different experimental methods can also produce seemingly contradictory results. A goal of this review is to summarize investigations of cadherin adhesion, in the context of functional data that must be accounted for by cadherin binding models. We emphasize, in particular, emerging parallels between diverse experimental findings and the evolving picture of the mechanism of cadherin adhesion. We also discuss seemingly disparate findings and their possible origins, and define future challenges towards developing a comprehensive model of cadherin adhesion that accounts for all of the experimental data.

4.2 Characteristics of Cadherin Binding

4.2.1 Trans *Cadherin Bonds*

We first consider functional signatures, which models of cadherin adhesion must capture, in order to account for the wide range of experimental data. First, cadherins

form *trans*, adhesive bonds with both similar and dissimilar classical cadherins on apposing cells. This is evidenced by classical cadherins' ability to promote the aggregation of nonadhesive cells when those cells are transfected with cadherins (Nose et al. 1988). Recombinant fragments of the ectodomains of *Xenopus* cleavage stage C-cadherin, epithelial E-cadherin, and neural N-cadherin all support cell adhesion to cadherin-coated substrata (Bixby and Zhang 1990; Brieher et al. 1996; Gavard et al. 2004; Pokutta et al. 1994). This capacity of isolated ectodomains to support the adhesion of cadherin-expressing cells or to aggregate beads demonstrates the adhesive function and localizes that function to the extracellular domain.

4.2.2 Cis-*Interactions and Cadherin Adhesion*

Several lines of evidence indicate that cadherins' adhesive function is also affected by their lateral organization on cell membranes. This organization occurs at two levels: namely, *cis* dimerization and the assembly of cadherins into larger scale clusters. Studies of soluble recombinant, ectodomains of C-cadherin as well as C-cadherin expressed on cells provided biochemical evidence for the existence of lateral dimers (Geng et al. 2004; Kim et al. 2005; Klingelhofer et al. 2002; Takeda et al. 1999; Troyanovsky et al. 2003). The functional significance of *cis* dimers was first demonstrated by biochemical studies in which dimers of C-cadherin ectodomains resulted in greater cell adhesion than did immobilized monomers (Brieher et al. 1996). Atomic force microscopy (AFM) and single molecule fluorescence imaging also identified dimers and larger 10–250 nm clusters on cell surfaces (Chtcheglova et al. 2010; Iino et al. 2001). These results suggested that lateral dimerization is one mechanism to enhance adhesion. It is unclear whether this is due to increased avidity, which results from an increase in the number of bonds formed, or to the allosteric enhancement of the intrinsic affinity of individual cadherin bonds.

The ability of C-cadherin fragments to form lateral dimers suggests that the ectodomain embeds a *cis* binding interface(s) (Brieher et al. 1996). However, a distinct interface that could mediate lateral-dimerization and account for different experimental data has yet to be identified. Potential contacts were identified in some structures (Sect. 4.3.2), but *cis*-dimers were not detected in biophysical studies of soluble extracellular domains. (Haussinger et al. 2002; Pokutta et al. 1994; Zhang et al. 2009).

Chemical cross-linking and immunoprecipitation results suggested that lateral and adhesive bonds may share the same interface (Troyanovsky et al. 2003). Inherent cadherin flexibility could enable cadherins to use the same binding interface for either *cis* or *trans* binding. The ectodomains are often portrayed as rigidly curved structures, but molecular dynamics simulations (Sotomayor and Schulten 2008) and electron microscopy images (He et al. 2003; Koch et al. 1999; Pokutta et al. 1994) indicate that, in the presence of calcium, the ectodomains can adopt other configurations than seen in the crystal lattice (Boggon et al. 2002).

Whether lateral dimerization is an intrinsic property of all classical cadherins remains to be established. The evidence so far suggests that some cadherins can form *cis*-dimers, but the distribution of cadherin monomers, dimers, and higher-order

aggregates is likely to be dynamic, and may depend on cell–cell adhesion. Cadherins also organize into much larger clusters on cell surfaces. Because extensive clustering requires Myosin II, Ena/VASP, and PIP3 (Gavard et al. 2004; Scott et al. 2006; Smutney et al. 2010), it is unlikely to be an intrinsic property of the cadherin structure, and will not be considered here.

4.2.3 Role of EC1 in Cadherin-Dependent Cell Adhesion

The importance of EC1 for cadherin adhesion was first demonstrated by studies in which exchanging EC1 domains of different cadherin subtypes altered cadherin-dependent segregation of cells that expressed different cadherins. In a cell-sorting assay, cells that expressed different cadherins at similar levels were shown to segregate away from one another in agitated cell suspensions, but the cells intermixed when they expressed the same cadherin (Nose et al. 1988). Specifically, cells expressing a chimeric protein, in which the EC1 domain of P-cadherin was replaced by the EC1 domain from E-cadherin, only formed aggregates with cells that expressed full-length P-cadherin (Nose et al. 1990). This localized the cell binding specificity to the N-terminal EC1 domain, and suggested that the identity of the EC1 domain was sufficient to specify cell aggregation patterns.

A variety of domain deletion analyses also supported the essential role of EC1 in cell adhesion (Chappuis-Flament et al. 2001; Shan et al. 2004). For example, substrata coated with domain deletion fragments that retained EC1-2 also support the adhesion of cells expressing C-cadherin (Chappuis-Flament et al. 2001). Additionally, cells expressing an N-cadherin mutant that only contained EC1-2 formed cell–cell aggregates (Shan et al. 2004).

4.2.4 Functional Evidence for Contributions from Other Regions of Cadherin Ectodomains

Experimental evidence suggests, however, that *trans*-binding between EC1 domains is not sufficient to account for the range of observed cadherin adhesive behavior. First, EC1 is necessary, but not sufficient, for cadherin-based cell adhesion. The EC1-2 region of N-cadherin appears to be the minimum fragment necessary for homophilic adhesion (Shan et al. 2004).

Second, genetic analyses of E-cadherin mutations associated with inherited gastric cancers identified clusters of mutations that are distributed along the entire extracellular domain, both within EC1 and outside of this domain in EC2-5 (Becker et al. 1999; Berx et al. 1998; Handschuh et al. 1999, 2001; Luber et al. 2000). Several of these mutants are expressed on the cell surface, but they impair cadherin's adhesive function to different extents (Becker et al. 1999; Berx et al. 1998). Intriguingly, several of the most deleterious mutations are within EC2 and EC3

(Fuchs et al. 2004; Handschuh et al. 1999, 2001; Luber et al. 2000). Mutations at the EC3-EC4 and EC4-EC5 junctions have a milder affect on adhesion (Handschuh et al. 1999, 2001; Prakasam et al. 2006a).

Third, aberrant glycosylation alters cadherin-specific cell functions including cell adhesion, barrier integrity, signaling, and interactions with the cytoskeleton (Geng et al. 2004; Guo et al. 2009; Jamal et al. 2009; Liwosz et al. 2006; Nita-Lazar et al. 2010; Pinho et al. 2009, 2011; Zhao et al. 2008a, b). In some cancers, abnormally high N-glycosylation of the membrane-proximal EC4 and EC5 domains of E-cadherin is associated with impaired intercellular adhesion and signaling. Mutating the eight N-glycosylation sites in the N-cadherin ectodomain increased the prevalence of dimers on cell membranes and enhanced ERK signaling (Guo et al. 2009). More limited mutagenesis localized N-glycosylation sites having the greatest impact on N-cadherin functions to EC2-3 (Jamal et al. 2009; Liwosz et al. 2006; Pinho et al. 2011; Zhao et al. 2008a).

Finally, cadherin blocking and activating antibodies have been identified that recognize membrane proximal EC domains. The E-cadherin blocking antibody DECMA-1 recognizes membrane proximal domains (Ozawa et al. 1990). An antibody that binds the EC5 domain of C-cadherin also activates strong *Xenopus* blastomere adhesion, and reverses the inhibitory effect of activin (Zhong et al. 1999).

These several lines of experimental evidence suggest that the entire ectodomain may contribute to cadherin's adhesive function in as yet incompletely understood ways. The following sections discuss structural and biophysical evidence for different cadherin interactions and possible mechanisms accounting for these experimental observations.

4.3 Structural Evidence for Cadherin Interactions

4.3.1 EC1-Domain Interactions

Structural studies of the extracellular domains (EC1-5) and of smaller fragments identified protein interactions responsible for many of the functional signatures discussed above. A consistently observed interface between EC1 domains in nearly all crystal structures of classical cadherins is termed the "strand swapped dimer" (Fig. 4.1b) (Katsamba et al. 2009). Essentially all biophysical and cell adhesion assays support the view that this is a *trans* adhesive bond. At this interface, tryptophan at position 2 (W2) inserts into a complementary hydrophobic pocket on EC1 of the apposing protein (Fig. 4.1b). Consistent with this being the central adhesive interface, mutating the conserved W2 residue to alanine (W2A) substantially reduces cell adhesion in a variety of assays (Pertz et al. 1999; Prakasam et al. 2006a; Shan et al. 2004; Tamura et al. 1998), however, W2A mutants localize to cell–cell junctions (Kitagawa et al. 2000; Tamura et al. 1998) and W2A fragments weakly aggregate beads (Prakasam et al. 2006a). Rotary shadowing electron micrographs of recombinant E-cadherin ectodomains also showed apparent association at the

N-terminal tips of the proteins (Pertz et al. 1999; Tomschy et al. 1996). Together, these experimental findings support the view that this EC1 interface mediates *trans* adhesion.

An additional contact seen in crystal structures of the EC1-2 fragment of E-cadherin, T-cadherin, and W2A mutants—termed the "X-dimer" (Fig. 4.1c)—is at the EC1-2 junction (Ciatto et al. 2010; Harrison et al. 2010; Nagar et al. 1996), where adjacent proteins interact through extensive nonpolar contacts between EC1 and EC2 domains in a tetrahedral configuration. An interface in the structure of E-cadherin EC1-2 (Nagar et al. 1996) was at first postulated to be a cloning artifact (Haussinger et al. 2004), but similar contacts in the structures of W2A mutants and of T-cadherin (Ciatto et al. 2010; Harrison et al. 2010) altered this view. The ability of mutations at this X-dimer interface to impede the rate of *trans*-dimerization led to the hypothesis that this complex is a transient intermediate in the kinetic pathway to strand dimerization (Harrison et al. 2010). T-cadherin also supports cell–cell adhesion (Ciatto et al. 2010), albeit more weakly than N-cadherin, indicating that this interface can also resist force.

4.3.2 Structures of Possible Cis *Binding Interfaces*

Evidence for *cis*-dimers has also been inferred from crystal packing interfaces and from electron microscopy images of ectodomains. A potential candidate for a *cis*-binding interface was observed in the structures of C-, E-, and N-cadherins (Boggon et al. 2002; Harrison et al. 2011). At this contact, EC1 contacts the EC2 domain of an adjacent protein in the crystal lattice (Boggon et al. 2002; Harrison et al. 2011). Mutations at this interface disrupt the organization of cadherin junctions (Harrison et al. 2011), thus supporting a role for this contact in cadherin ordering at junctions. Interactions between amino acids within this interface were not, however, confirmed by NMR measurements of E-cadherin EC1-2 (Haussinger et al. 2002), by electron micrographs of cadherin ectodomains (Pokutta et al. 1994), or by single-molecule fluorescence measurements (Zhang et al. 2009), indicating that the dissociation constant (K_d) exceeds 1 mM (Harrison et al. 2011). Other contacts in crystal lattices that were originally attributed to *cis* interactions include calcium bridging at the interdomain junction between parallel E-cadherin EC1-2 fragments (Nagar et al. 1996). In hindsight, this structure was found to be the X-dimer (Fig. 4.1c). Mutating acidic calcium-binding residues at this junction disrupts adhesion (Prakasam et al. 2006b), although this could be due to perturbations of the X-dimer intermediate or to allosteric perturbation of W2 docking (Harrison et al. 2005; Haussinger et al. 2002; Sotomayor and Schulten 2008; Vunnam and Pedigo 2011b). Another potential *cis* bond involves EC4, which is required for the oligomerization of soluble VE-cadherin ectodomains (Bibert et al. 2002; Hewat et al. 2007; Lambert et al. 2005; Taveau et al. 2008). Intriguingly, only non-glycosylated VE-cadherin appears to form hexamers (Brasch et al. 2011).

In addition to structure determinations, several other biophysical approaches were used to interrogate cadherin function and to test models for cadherin-based cell adhesion. These can be divided generally into solution-binding and adhesion measurements. In solution, freely diffusing cadherins associate under force-independent conditions, but in adhesion measurements, cadherins are confined to surfaces and subject to force, as they would be at cell–cell junctions. Adhesion-based approaches provide complementary information about the number, dynamics, and strength of cadherin bonds. Sections 4.4 and 4.5 describe experimental results obtained with different biophysical methods, and discuss results in the context of structures and of cell adhesion.

4.4 Solution Studies of Cadherin Ectodomain Interactions

4.4.1 Analytical Ultracentrifugation (AUC) Measurements of Binding Affinities

Affinity differences that are at the heart of type I classical cadherin interactions have been characterized using *Sedimentation Equilibrium* and *Sedimentation Velocity* experiments by Analytical Ultra Centrifugation (AUC). AUC can be used to characterize the hydrodynamic and thermodynamic properties of macromolecules in solution, by monitoring their sedimentation in a centrifugal field (Lebowitz et al. 2002). In *sedimentation equilibrium* experiments, at small centrifugal forces, an equilibrium is established where sedimentation is balanced by diffusional transport. Analysis of this sedimentation equilibrium yields information on the molar mass of the proteins, their states of association, and the free energies of binding (Lebowitz et al. 2002). Alternatively, in a *sedimentation velocity* experiment, a larger centrifugal force causes rapid protein sedimentation. Although sedimentation velocity experiments cannot determine binding affinities, analysis of the evolving concentration gradients can be used to determine whether the kinetics is fast or slow relative to the time-scale of the experiment (Lebowitz et al. 2002). In contrast to surface plasmon resonance (SPR) and other dynamic approaches described below, sedimentation velocity AUC cannot yield quantitative rate constants, but instead qualitatively assesses whether the molecules exchange rapidly or slowly within a ~45 min period.

Sedimentation equilibrium AUC measurements of the dissociation constant (K_d) of wild type and mutant classical cadherin homodimerization are summarized in Table 4.1. These measurements focused on two-domain protein constructs (EC1-2), except for the full-length ectodomain of C-cadherin (EC1-5), for which the determined K_d for homodimerization was 64 μM (Table 4.1) (Chappuis-Flament et al. 2001). Wild type E-cadherin EC1-2 expressed in mammalian and in bacterial cells have similar affinities with K_d values of 97 μM (Katsamba et al. 2009) and 80 μM (Koch et al. 1997), respectively. Sedimentation equilibrium AUC experiments also show that the solution binding affinity for N-cadherin EC1-2 is fourfold higher than

Table 4.1 AUC measurements of the dissociation constants for cadherin homodimerization

Protein	Description	Mean K_d (μM)	References
C-cadherin EC1-5 construct			
WT	Wild type	64	Chappuis-Flament et al. (2001)
E-cadherin EC1-2 constructs			
WT	Wild type	80 ± 20	Koch et al. (1997)
WT	Wild type	96.5 ± 10	Katsamba et al. (2009)
WT	Wild type	98.6 ± 15	Ciatto et al. (2010)
W2A	Strand-swap mutant	916 ± 47	
Ala-Ala N-terminal extension	Strand-swap mutant	811 ± 97	
E89A	Strand-swap mutant	293 ± 11	
Asp-Trp deletion at N-terminus	Strand-swap mutant	662 ± 28	Harrison et al. (2010)
K14E	X-dimer mutant	117 ± 8	
K14S	X-dimer mutant	96.0 ± 1.0	
Y142R	X-dimer mutant	77.4 ± 1.4	
W2A K14E	Double mutant	Monomer	
W2F	Reduced strain on A*/A strand	246 ± 2	Vendome et al. (2011)
A inserted between 2 and 3	Reduced strain on A*/A strand	1,517 ± 726	
AA inserted between 2 and 3	Reduced strain on A*/A strand	195 ± 8.6	
E11D	Enhanced strand-swapping	71 ± 12	
W2F	Reduced strain on A*/A strand	246 ± 2	
P5A P6A	Alternate interface	3.7 ± 0.1	
P5S P6S	Alternate interface	2.9 ± 0.04	
P5G P6G	Alternate interface	2.7 ± 1.68	
P5A	Alternate interface	2.9 ± 2.1	
P6A	Alternate interface	4.8 ± 1.65	
N-cadherin EC1-2 constructs			
WT	Wild type	25.8 ± 1.5	Katsamba et al. (2009)
P5A P6A	Alternate interface	3.6 ± 0.2	Vendome et al. (2011)

the E-cadherin EC1-2 at 25°C (Table 4.1) (Katsamba et al. 2009). It is noteworthy that a fourfold difference is not large relative to the thermal energy, amounting to only ~0.8 kcal/mole at 37°C. Such differences would, however, be amplified by large numbers of cadherin bonds at junctions.

Sedimentation equilibrium AUC measurements also determined the binding affinities of cadherin mutants that abolish strand swapping. Mutating the conserved W2 to Ala (W2A) significantly increases the K_d to 916 μM (Table 4.1) (Harrison et al. 2010). Similarly, strand swapping is stabilized by the formation of a salt bridge between the side chain of Glu89 and the N-terminus of the swapped strand. Extending the N terminus (Ala-Ala–extension mutant) or replacing Glu89 with an

uncharged residue (E89A) eliminates this salt-bridge. Relative to wild type, these mutants increased the K_d values to 811 and 293 μM, respectively (Harrison et al. 2010). Finally, abolishing the strand swapping entirely, by deleting two N-terminal residues ('Asp-Trp deletion' mutant), which removes the entire swapped structural element, increased the K_d to 662 μM (Table 4.1) (Harrison et al. 2010).

Mutations that relieve strain in the swapping strand in cadherin monomers also decrease the dimerization affinity because the short, swapping-strand in the closed-monomer is strained. This is due to its anchorage at one end by the conserved W2 and at the other by a Ca^{2+}-Glu11 ion pair. This conformational strain provides the driving force for strand expulsion and swapping (Vendome et al. 2011). Mutating the conserved W2 to Phe (W2F) decreases strain in the monomer, and increases K_d to 246.5 μM (Table 4.1) (Vendome et al. 2011). Similarly, increasing the length of the swapping strand reduces strain, such that inserting one or two alanines increases the K_d values to 1,517 and 195 μM, respectively (Table 4.1) (Vendome et al. 2011). On the other hand, increasing the strain by shortening the Glu11 side-chain, while preserving the Ca^{2+}-binding site (E11D mutant), reduces the K_d slightly to 71.2 μM (Table 4.1) (Vendome et al. 2011).

A conserved proline-proline motif in the swapped strand ensures that the cadherin pair cannot form a continuous hydrogen-bonded β-sheet (Vendome et al. 2011; Vunnam and Pedigo 2011a), such that mutating Pro5, Pro6, or both results in an unnaturally tight dimer. With such E-cadherin mutants, the *trans* dimerization K_d value decreases by almost two orders of magnitude (Table 4.1) (Vendome et al. 2011), and the P5AP6A double mutant similarly decreases the N-cadherin EC1-2 K_d (Vendome et al. 2011). Notably, despite the fourfold difference in affinity between the wild-type proteins, the K_d values of the double mutants of E- and N-cadherin are essentially identical (Vendome et al. 2011).

In contrast to strand-swapping mutants, AUC experiments show that mutants that cannot form X-dimers have K_d values that are virtually indistinguishable from wild type protein (Table 4.1) (Harrison et al. 2010). This suggests that the thermodynamics of strand dimerization is not substantially affected by X-dimer interface mutations (Harrison et al. 2010), which instead primarily affect the rate of equilibration. Sedimentation velocity AUC experiments showed that the wild-type protein shows sedimentation behavior characteristic of rapidly exchanging monomer-dimer equilibrium, whereas the X-dimer mutants exhibit a slowly exchanging equilibrium, where little inter-conversion between monomers and dimers occurs on the measurement timescale (~45 min) (Harrison et al. 2010).

4.4.2 Surface Plasmon Resonance (SPR) Measurements of Relative Binding Affinities

Surface Plasmon Resonance (SPR) (Homola 2008) measurements compared relative homophilic and heterophilic K_d values of classical cadherins (Katsamba et al. 2009). SPR quantifies the time-dependent change in ligand binding to immobilized

receptors, as ligand solution is flown over the receptor-coated sensor chip. From these data, one can obtain association and dissociation rates, as well as the affinities for simple receptor-ligand binding. However, determinations of affinities between molecules that also dimerize in solution are complicated by the two competing equilibria. Obtaining quantitative homophilic cadherin K_d values required more complicated analyses of binding kinetics and equilibria, so that it was only possible to determine relative dissociation constants (Katsamba et al. 2009). In agreement with the AUC measurements (Table 4.1), the homophilic dimerization K_d of N-cadherin EC1-2 was lower than the K_d of E-cadherin EC1-2 (Katsamba et al. 2009). The relative K_d for the heterophilic interaction between N- and E-cadherin is intermediate between the homophilic values (Katsamba et al. 2009).

SPR measurements similarly explored the effect of strand-dimer and X-dimer mutations on cadherin K_d values (Harrison et al. 2010). Although wild type E-cadherin EC1-2 forms homo-dimers, the K14E X-dimer mutant does not interact with either the immobilized K14E mutant or the wild type protein (Harrison et al. 2010). In agreement with sedimentation velocity AUC experiments, this suggests that the association rate for the dimerization of X-dimers mutants is very slow (Harrison et al. 2010).

4.4.3 Single-Molecule Fluorescence Measurements of Classical Cadherin Conformation

Fluorescence-based techniques like Förster Resonance Energy Transfer (also known as Fluorescence Resonance Energy Transfer or FRET) (Roy et al. 2008) and sub nanometer single-molecule localization (Pertsinidis et al. 2010) have been used to measure the conformation of pairs of isolated cadherin molecules. In a FRET experiment, the cadherins are tagged on a specific EC domain with one of two fluorescent dyes, called donor and acceptor dyes respectively (Figs. 4.2a, c). The cadherins are allowed to interact and the distance between the fluorescent probes is measured with nanometer resolution. Dyes separated by more than ~10 nm do not interact, and the donor emits photons upon its excitation by laser. However if the two dyes are closer than ~10 nm, then the donor transfers its energy to the acceptor, which emits photons of a different wavelength. By monitoring the relative intensities of the donor and acceptor fluorescence, nanometer scale distance changes can be resolved (Roy et al. 2008). In single-molecule localization, fluorescent dyes are attached to a specific EC domain, the position of the dyes are localized with sub nanometer resolution, and the distance between these domains in the cadherin complex is determined (Pertsinidis et al. 2010).

Single molecule FRET measurements between soluble cadherins labeled on the N-terminal domain (Fig. 4.2a) showed that, in the presence of Ca^{2+}, a majority of cadherin monomers homodimerize via their EC1 domains (Fig. 4.2b) (Zhang et al. 2009). Since these experiments could not differentiate between cadherins interacting in *cis* or in *trans* orientations, recombinant dimers were engineered to

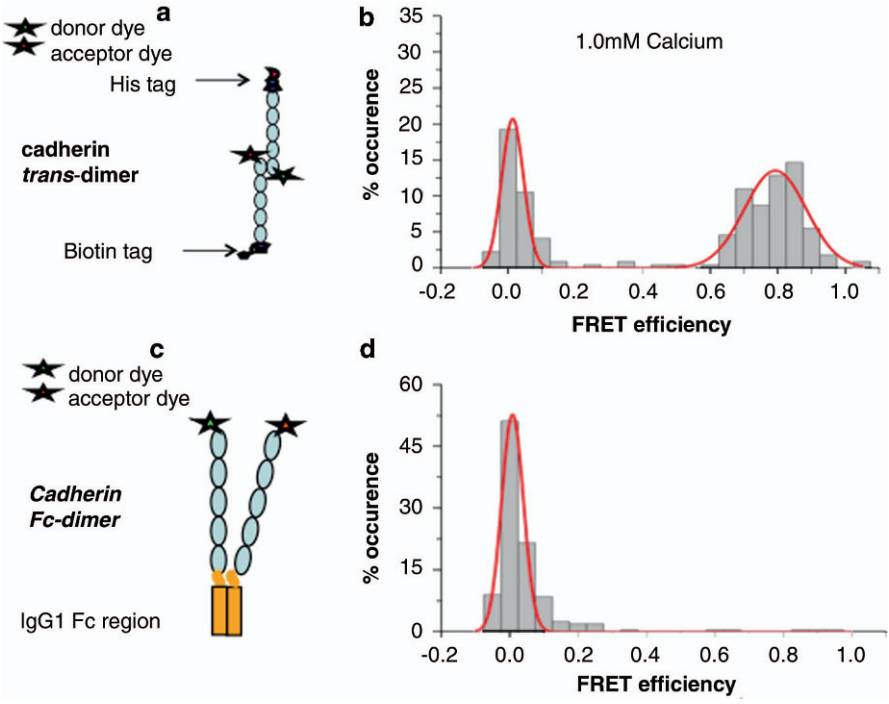

Fig. 4.2 Adapted from (Zhang et al. 2009). **a** *Trans*-dimers formed between E-cadherin monomers fluorescently labeled on the EC1 domains. **b** The majority of *trans*-dimers in 1.0 mM Ca^{2+} exhibit a FRET value of 0.8, which corresponds to a distance of 4 nm between EC1 domains. **c** Fluorescently labeled E-cadherins placed in a close *cis* orientation (cadherin-Fc dimer construct). **d** E-cadherin-Fc dimers in 1.0 mM Ca^{2+} exhibit very few events with a FRET efficiency above 0.5, indicating that these proteins do not form a *cis* bond

force the ectodomains into a close *cis*-orientation (Chappuis-Flament et al. 2001). The outermost domain of the resulting *cis* dimers were then dual-labeled with donor and acceptor fluorophores (Fig. 4.2c), and the distance between them was monitored by FRET. In this case, the FRET signals indicated that, although the cadherins were in close proximity, they did not interact in *cis* (Fig. 4.2d) (Zhang et al. 2009).

Similar studies investigated the reaction pathway for *trans* dimerization (Sivasankar et al. 2009). Two alternative pathways for tryptophan exchange have been proposed (Miloushev et al. 2008). In the induced-fit pathway, cadherin monomers with buried W2 residues, form a W2-independent, initial encounter complex (Fig. 4.1c). Subsequent conformational changes result in W2 strand swapping. In the selected-fit pathway, cadherin monomers adopt an "active" conformation that exposes the W2 residues before binding. Subsequent collisions between "activated" cadherin monomers result in the formation of a stand-swapped dimer. In order to resolve these questions regarding the strand exchange mechanism, the W2A mutant was used to block the selected-fit pathway (Sivasankar et al. 2009). Thus individual W2A mutants would only interact, if the cadherins dimerized via an induced-fit

mechanism. Because W2A mutants cannot proceed to the strand-swapped dimer, this strategy kinetically captured the initial encounter complex, which was detected and characterized by single molecule FRET. This result strongly suggests that cadherins initially interact via their outermost domains to form an initial encounter complex (Sivasankar et al. 2009), which is likely to be the X-dimer.

An ultra-stable, sub nanometer, single-molecule localization microscope was recently used to measure inter subunit distances of E-cadherin dimers cross-linked in solution (Pertsinidis et al. 2010). The EC5 domain of the cadherins was labeled with fluorescent dye and the distance between the EC5 domains was measured. In the presence of Ca^{2+}, a majority of E-cadherin dimers adopted an extended *trans*-conformation (EC5-EC5 distance = 32.2 nm) (Pertsinidis et al. 2010), consistent with the crystal structure of the C-cadherin ectodomain (Boggon et al. 2002). A smaller population had an EC5-EC5 distance of ≈ 25 nm, which may be an alternative conformation due to flexibility of the dimer complex and/or association of the inner domains. In agreement with single molecule FRET and NMR studies (Haussinger et al. 2002; Zhang et al. 2009), there was no evidence for *cis*-dimerization in solution (Pertsinidis et al. 2010).

4.5 Adhesion Based Studies of Cadherin Interactions

The capacity for cadherin bonds to resist force is a central function of classical cadherins such that adhesion-based measurements provide additional, functionally relevant information about the dynamics and strengths of cadherin bonds. The physics of the force-dependent rupture of noncovalent, bonds enables determinations of different dynamic and physical properties of protein bonds that complement force-independent measurements such as solution binding affinities (Sect. 4.4). Mechanical measurements use force to accelerate bond failure, and the rupture force (bond strength) reflects the activation energy for unbinding, intrinsic dissociation rate, and the shape of the interaction potential (Dudko 2009; Dudko et al. 2006, 2008; Evans and Ritchie 1997). Force measurements can also quantify protein-mediated adhesion energies directly (Leckband and Israelachvili 2001). The principals of typical force measurement approaches and the information they provide are reviewed elsewhere (Evans 1998; Evans and Calderwood 2007; Leckband and Israelachvili 2001).

4.5.1 Surface Force Apparatus Measurements

The surface force apparatus quantifies the interaction energy between two surfaces, as a function of the separation distance, within ±0.1 nm (Israelachvili 1992; Israelachvili and Adams 1978; Leckband and Israelachvili 2001). This approach has been used extensively to study the interactions of several proteins (Johnson

et al. 2004, 2005b; Leckband et al. 1995a, b, 2011; Leckband and Prakasam 2006; Menon et al. 2009; Sivasankar et al. 1998, 2001; Yeung et al. 1999; Zhu et al. 2003), including cadherins. In several examples, including CD2, CD58, antibodies, streptavidin, the immune proteins DC-SIGN and DC-SIGNR, cytochrome b5 and cytochrome c, and the protein dimensions measured with this approach agreed quantitatively with crystallographic data (Bayas et al. 2007; Johnson et al. 2004, 2005a; Leckband 2000; Leckband et al. 1994, 1995b, 2011; Yeung et al. 1999; Zhu et al. 2002).

Surface force measurements of the distance-dependence of interactions between opposing cadherin monolayers identified three main features of cadherin binding. First, the measurements identified three distinct cadherin bonds that require different EC domains (Sivasankar et al. 2001; Zhu et al. 2003). Second, they quantified differences between adhesion energies of cadherin subtypes (Prakasam et al. 2006b). Third, they demonstrated that cadherin subtypes cross-react with heterophilic adhesion energies that are intermediate between those of homophilic bonds (Leckband and Prakasam 2006; Prakasam et al. 2006b). Further investigations explored the impact of cancer-associated, calcium-site mutations (Prakasam et al. 2006a) and of *N*-glycosylation (unpublished) on cadherin adhesion.

The distance dependent force between oriented monolayers of C- and N-cadherin ectodomains immobilized on supported lipid membranes (Fig. 4.3a) detected three adhesive interactions that occur at three, distinct membrane separations (Fig. 4.3b). These three cadherin adhesions were separated by ~4 nm—the length of one EC domain (Prakasam et al. 2006b; Zhu et al. 2003). Although the existence of multiple adhesive bonds was initially unexpected, two of the three bonds identified are consistent with current structural data. Adhesion at the membrane separation of 39 nm requires EC1 (Zhu et al. 2003) and W2 (Shi et al. 2010), and is at a distance consistent with a strand-swapped dimer under tension (Sotomayor and Schulten 2008). Adhesion at the separation of 32 nm requires EC1-2, but not W2 (Shi et al. 2010), and is at a distance that is geometrically consistent with the X-dimer complex (Fig. 4.3b) (Hong et al. 2011). The third and strongest adhesion measured under these conditions requires EC3, and is at a membrane distance (26 nm) at which EC3 domains could interact directly.

Studies of the impact of cancer-associated mutations at calcium binding sites in E-cadherin revealed the functional consequences of mutations far from the EC1 domain in the cadherin sequence. Alanine substitutions at D103 and D134 in EC1-2 of E-cadherin ablated EC1-EC1 adhesion and reduced EC3-dependent adhesion (Prakasam et al. 2006a). In comparison with the X-dimer structure and with solution binding studies of N-cadherin D103A and D134A mutants (Prasad and Pedigo 2005; Vunnam and Pedigo 2011b), the D103A mutant likely inhibits X-dimer formation: this mutant retains the interdomain structure but does not form the strand swapped dimer (Vunnam and Pedigo 2011b). The D134A mutant abolishes all calcium binding at the junction and hence the X-dimer intermediate (Prakasam et al. 2006a; Vunnam and Pedigo 2011b), but the effect of these mutations on EC3-dependent adhesion also suggests that these perturbations affect distant sites in the protein. These findings provided evidence for long-ranged

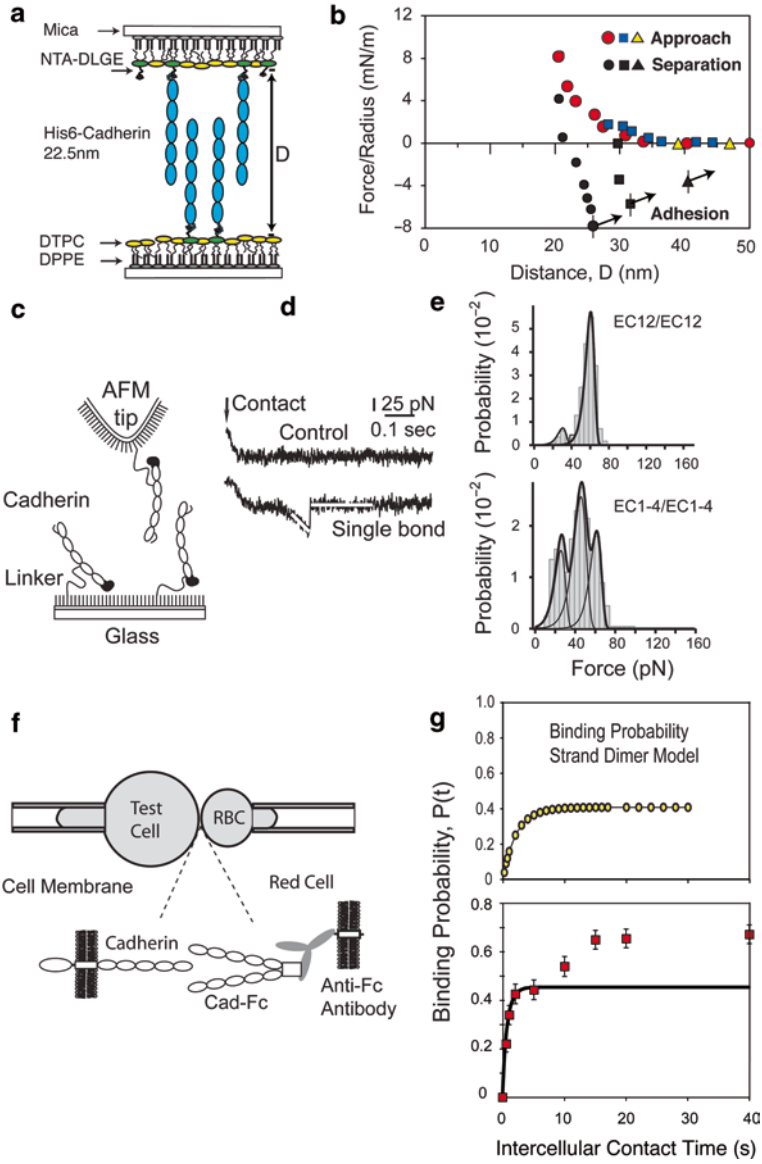

Fig. 4.3 Summary of force-based measurements of cadherin interactions. **a** Sample configuration used in surface force measurements. The distance, D, is the separation between lipid membranes. C-cadherin extracellular domains with C-terminal His tags were immobilized on supported lipid bilayers. The outer membrane leaflet contains di-lauryl glycerol ester (*DLGE*) with nitrile-tri-acetic-acid head groups (*NTA-DLGE*) mixed with di-lauryl-phosphatidyl-choline (*DLPC*). The lipid adjacent to the mica is di-lauryl-phosphatidyl-ethanolamine (*DLPE*). **b** Force normalized by the radius of the curved substrate, F/R versus the distance between the membranes. Forces were measured during approach (*colored symbols*) and during separation (*black symbols*). The outward directed arrows indicate the three distinct positions at which the ectodomains adhere, and the

inter-domain cooperativity, which could play a role in propagating binding information to the cytoplasmic domain.

Consistent with long-range interdomain cooperativity, the D216A mutation at the EC2-3 junction (Handschuh et al. 1999, 2001) is far from all postulated *trans* and *cis* binding interfaces, but it reduces cell–cell adhesion, increases migration, and is associated with aggressive metastatic gastric tumors (Becker et al. 1999; Handschuh et al. 1999, 2001). This mutation did not significantly perturb the E-cadherin ectodomain structure (Prakasam et al. 2006a), but it eliminated EC1-EC1 adhesion and significantly weakened the EC3-dependent bond. This both demonstrated the protein-level impact of these mutations on cell adhesion and demonstrated the long-ranged structural effect of the perturbations.

Taken together, the force-distance measurements identified distinct, adhesive interactions at different membrane distances that require different EC domains (Fig. 4.3b). Except for the EC3-dependent interaction, two of these adhesions are compatible with existing structural and solution binding data. The outermost bond is the strand-swapped dimer: it requires W2 and fails at the membrane separation compatible with the complex under tension (Sotomayor and Schulten 2008). The existence of additional interactions beyond EC1 was initially controversial, but the bond at the intermediate distance is geometrically consistent with the recently identified X-dimer (Hong et al. 2011; Leckband and Prakasam 2006).

Homophilic adhesion energies attributed to the strand-swapped dimer between chicken N-, canine E-, and *Xenopus* C-cadherin ectodomains differed by at most fourfold. Homophilic E-cadherin adhesion exceeded N-cadherin adhesion, and differs from relative solution binding affinities (Katsamba et al. 2009). However, these adhesion data were corroborated by single molecule measurements (Shi et al. 2008) (Sect. 4.5.2) and by measured cadherin affinities at the cell surface (Sect. 4.5.3). The difference in relative magnitudes of E- and N-cadherin adhesion in the context of solution binding data could be due to sequence differences between the cadherin subtypes used.

Heterophilic interactions similarly exhibited multiple adhesive bonds at quantitatively identical spacing as the homophilic bonds (Prakasam et al. 2006b). The quantified EC1-dependent adhesion energies were intermediate between those of

---

pull-off force, indicated by the outward directed arrows, gives the adhesion. **c** AFM set up showing the probe tip and substrate with sparsely immobilized cadherin ectodomains. **d** Force versus tip-surface separation curves in an AFM measurement. In the absence of adhesion, the trace is flat (*top*), but the formation of a single bond causes the force to increase (*dip*) and then snap back to zero at bond rupture. **e** Force histograms measured between EC12 (*top*) and EC1-4 (*bottom*) fragments. The solid lines are Gaussian fits to models for two (*top*) and three bonds (*bottom*). **f** Micropipette manipulation experiment. Two cells are aspirated into apposed pipettes (*top*) and then repetitively brought in and out of contact. The test cell expresses cadherin (*bottom*). A red blood cell is covalently modified with monoclonal anti-Fc antibody, which captures Fc-tagged cadherin dimers (*bottom*). **g** Binding probability time courses. The top panel shows the theoretical binding probability for the strand swapping mechanism. The cadherin binding kinetics exhibit a fast initial rise to P ~ 0.5, followed by a 2–5 s lag, and a second rise to a higher binding probability at P ~ 0.7. The solid line through the data is the fit of the first binding step to the strand-swap mechanism

the homophilic bonds (Prakasam et al. 2006b), as was later also shown qualitatively by SPR (Katsamba et al. 2009).

4.5.2 Single Molecule Bond Rupture Measurements

Single molecule AFM measurements quantify the forces to rupture single protein-ligand, e.g. cadherin-cadherin bonds as a function of the rate at which the bonds are pulled. In measurements with cadherins, the proteins are attached to the small tip of a cantilever in the AFM and to an opposing surface (Fig. 4.3c). Sparsely immobilized proteins adhere when the cantilever is brought into contact with sparse proteins on the test surface, and retracting the cantilever increases the force on the bond, until it fails (Fig. 4.3d). Bond rupture events are stochastic, so that histograms of rupture forces are generated from hundreds of measurements (Fig. 4.3e). In typical bond rupture measurements, referred to as force spectroscopy, the most probable rupture force depends on the rate of pulling, the bond dissociation rate, and the distance between the ground state and the transition state (Dudko 2009; Dudko et al. 2006; Evans and Ritchie 1997; Suzuki and Dudko 2010). Analyses of these force histograms determine the number of distinct bonds formed, their strengths, and the bond dissociation rates (Dudko 2009; Dudko et al. 2006, 2007, 2008; Evans 2001; Evans and Ritchie 1997, Evans and Calderwood 2007). Alternatively, bond lifetimes determined under constant force ("force-clamp") generate similar, complementary information (Bayas et al. 2006). Four, independent research groups used single molecule force measurements to investigate both homophilic and heterophilic cadherin interactions (Baumgartner et al. 2000; Bayas et al. 2006; du Roure et al. 2006; Perret et al. 2004; Shi et al. 2008, 2010; Tsukasaki et al. 2007).

Single molecule studies mainly compared binding characteristics of EC1-5, EC domain deletions, and W2A mutants of different classical cadherins. Findings with EC1-2 fragments are consistent with solution-based measurements, cadherin structures, and force-distance measurements. E-cadherin forms multiple, independent bonds with a hierarchy of strengths and dissociation rates (Perret et al. 2004). Force histograms measured between EC1-2 fragments of C-cadherin or E-cadherin identified two, weak bonds with fast dissociation rates (Fig. 4.3e, top) (Bayas et al. 2006; Perret et al. 2004; Shi et al. 2010). One of the bonds requires W2 (Shi et al. 2010).

In light of structural data, the W2-independent interaction is likely the X-dimer. The measured strength of the putative X-dimer is ~25% that of the strand swapped dimer, when the rupture forces were quantified at similar pulling rates (Sivasankar et al. 2009). Force spectroscopy measurements (Sect. 4.4) also indicate that the W2-independent bond is weaker, at the pulling rates examined (Shi et al. 2010). However, further studies at different forces and with different proteins, e.g. K14E X-dimer mutant would conclusively define the kinetic and mechanical properties of these two EC1-2 bonds.

In addition to the two, EC1-2 dependent bonds, force histograms measured with full length EC1-5 domains of canine, human, and mouse E-cadherin (Perret et al.

2004; Shi et al. 2008; Tsukasaki et al. 2007), chicken N-cadherin (Shi et al. 2008), and *Xenopus* C-cadherin (Bayas et al. 2006; Shi et al. 2008) form an additional, stronger bond with a slow dissociation rate. *Xenopus* C-cadherin EC1245, which lacks EC3, only exhibited two weak, fast bonds as observed with EC1-2, suggesting that this third interaction requires EC3 in some way (Shi et al. 2010). This result corroborated surface force measurements with the same proteins (Shi et al. 2010; Zhu et al. 2003). AFM measurements of C-cadherin domain deletion mutants EC1-3, EC1-4, and EC1-5 also exhibited three, distinct peaks in force histograms (Fig. 4.3e, bottom) (Shi et al. 2010). The strength of the third, additional interaction increases with the ectodomain length (Shi et al. 2010), indicating that EC4 and EC5 augment this third bond, possibly by stabilizing the binding interface.

4.5.3 Kinetic Measurements of Cadherin-Mediated Cell–Cell Binding

An alternative approach to both force measurements and solution-binding studies uses micropipette manipulation to quantify the kinetics of binding between single cells that are partially aspirated into apposing micropipettes (Fig. 4.3f). The intercellular binding probability is the number of cell–cell binding events divided by the total number of times the cells are repetitively brought into contact, and reflects the number of intercellular bonds (Chesla et al. 1998). The time-dependence of the binding probability depends on the binding mechanism, the kinetic rates and affinities, the contact time, and the cell–cell contact area (Chesla et al. 1998). The two-dimensional affinities and dissociation rates of adhesion proteins on the cell membrane are determined from fits of the data to kinetic rate equations that describe mathematically the postulated binding mechanism. Such measurements determined the two-dimensional affinities and kinetic rates for several proteins, including selectins, T-cell/MHC, integrins, MHC/CD8, and C-cadherin (Chen et al. 2008; Chesla et al. 2000; Chien et al. 2008; Huang et al. 2004, 2007, 2010; Long et al. 2001; Piper et al. 1998; Williams et al. 2001; Zhang et al. 2005).

For simple receptor-ligand interactions such as the strand swapping mechanism, the binding probability is described by a simple exponential that rises smoothly to a limiting plateau (Fig. 4.3g, top) (Chien et al. 2008). However, the binding kinetics of *Xenopus* C-cadherin occurs in two stages: an initial fast step with a low binding probability is followed by a lag or induction phase and then a subsequent rise to a second, higher binding probability (Fig. 4.3g, bottom) (Chien et al. 2008). This kinetic signature was measured with *Xenopus* C-cadherin (Chien et al. 2008); human and canine E-cadherin; chicken, mouse, and human N-cadherin (unpublished). Similar results were obtained for both homophilic and heterophilic binding.

C-cadherin domain deletions identified domains necessary for the two kinetic steps. The C-cadherin EC1-2 and EC1245 fragments only displayed the fast, initial binding step (Chien et al. 2008), which is attributed to strand swapping. The strand exchange model also describes the EC12 and EC1245 kinetic profiles and the

Table 4.2 Two dimensional homodimerization affinities and dissociation rates from cell binding kinetics

Cadherin on Test Cell	Density (#/μm^2)	Cadherin-Fc on Red Cell	Density (#/μm^2)	2D Affinity ($\times 10^{-4}$ μm^2)	Dissociation rate (s^{-1})
C-cadherin	18	C-cadherin	10	11±2	0.6±0.2
C-cadherin	7	C-EC1245	10	30±9	0.3±0.1
C-cadherin	7	C-EC12	155	1.4±0.5	0.9±0.2
C-cadherin W2A	24	C-cadherin	452	0.12±0.05	0.10±0.03
N-cadherin	15	N-cadherin	69	1.9±0.3	1.1±0.4
E-cadherin	16	E-cadherin	44	3.3±0.5	1.0±0.3
C-cadherin	14	N-cadherin	38	3.5±0.2	1.3±0.3
C-cadherin	18	E-cadherin	33	3.3±0.9	1.3±0.4
N-cadherin	16	E-cadherin	33	2.6±0.4	1.2±0.5

first binding step measured with EC1-5 (Fig. 4.3g, bottom). Model fits to the data thus determine the two-dimensional (2D) binding affinity and dissociation rates for EC1-EC1 bonds (Table 4.2). The EC12-dependent affinities for EC1245 and EC1-5 were identical, but the EC1-2 affinity was ~20 fold lower. The latter difference may be partly due to protein length differences, which affect two-dimensional affinities (Huang et al. 2004). The W2A mutation altered the kinetic profile relative to the wild type protein, and the residual binding affinity, which is presumably due to X-dimerization, was ~100 fold lower (Chien et al. 2008) (Table 4.2).

Studies of C-cadherin domain deletion mutants showed that EC3 is necessary for the second rise to the high probability state observed with EC1-5. This kinetic profile cannot be described by a proposed transient intermediate (Harrison et al. 2010), suggesting that a different mechanism, possibly involving *cis* interactions, underlies this behavior. Consistent with this notion, a glycosylation mutant that alters the prevalence of N-cadherin dimers on the cell surface (Guo et al. 2009) also changes the kinetics in a manner suggesting that the second step involves lateral dimerization (unpublished). Kinetic analyses also suggest that initial cell–cell binding nucleates the second step. These findings are qualitatively consistent with recent simulations, which suggest that initial *trans* binding facilitates *cis* dimerization in intermembrane gaps (Wu et al. 2010, 2011).

4.6 Conclusions and Future Directions

Accumulating experimental data are revealing several parallels between structures, solution-binding data, and adhesion measurements that reconcile in part what previously appeared to be contradictory findings (Fig. 4.4). The EC1-2 domains are the most extensively studied fragments, and studies provide the greatest qualitative agreement among different experimental measurements. All approaches identified a W2-dependent interaction between EC1 domains that is consistent with the strand-swapped dimer. Single molecule AFM, surface force measurements, FRET, and

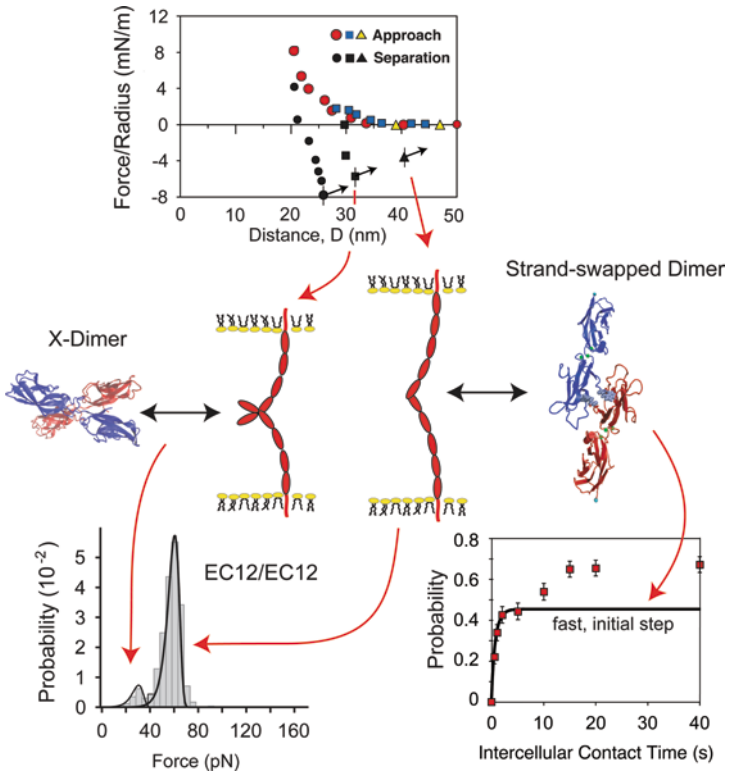

Fig. 4.4 Comparison of current biophysical and structural data. The structures of the *trans* and X-dimers (*center*) are compared with cadherin binding signatures from three different biophysical measurements discussed in the text. The *red arrows* highlight the correspondence between solution binding and/or geometrical/structural characteristics of the *trans* or X-dimer (*center*) and the different features in surface force measurements (*top*), AFM data (*bottom left*), and cell binding kinetics (*bottom right*)

intercellular binding kinetics also identified a W2-independent interaction between EC1-2 fragments (Bayas et al. 2006; Chien et al. 2008; Harrison et al. 2010; Perret et al. 2004; Prakasam et al. 2006a; Shi et al. 2010; Sivasankar et al. 2009), which is consistent with the X-dimer interface (Ciatto et al. 2010; Harrison et al. 2010). The W2-independent middle bond detected in force-distance measurements is geometrically consistent with the X-dimer (Hong et al. 2011; Shi et al. 2010; Sivasankar et al. 2001; Zhu et al. 2003). As summarized below, some differences remain. We discuss studies that may further reconcile the diverse observations discussed in this chapter, and generate a comprehensive functional and structural understanding of classical cadherins.

First, one apparent difference between experimental results is the low affinity and short lifetime of the X-dimer measured under force-independent conditions (Harrison et al. 2010) compared with surface force measurements (Bayas et al. 2006; Leckband and Sivasankar 2000; Perret et al. 2004; Shi et al. 2010). There

are, however, increasing examples of differences between equilibrium binding and adhesion-based measurements, most notably in the case of catch bonds, which have no apparent strength in the absence of force but strengthen when pulled (Marshall et al. 2003; Thomas 2008, 2009; Zhu et al. 2008). The adhesive behavior of catch bonds, rather than the solution binding affinity, is the functionally relevant property (Marshall et al. 2003; Thomas 2008, 2009; Zhu et al. 2008). It will be interesting to determine whether cadherins also exhibit catch bond behavior.

A second issue concerns the existence of a unique *cis* dimer interface and the possible role(s) of domains other than EC1-2. A *cis* interface that was postulated on the basis of several crystal structures (Harrison et al. 2011), was not confirmed by solution NMR (Haussinger et al. 2002), electron microscopy (Pokutta et al. 1994), or fluorescence (Zhang et al. 2009). By contrast, a possible role for EC3-5 is supported by biophysical data, and could explain the impact of *N*-glycosylation mutants on *cis* dimerization (Guo et al. 2009). A functional interface involving EC3-5 could also account for the effect of D216A at the EC2/EC3 junction on adhesion (Handschuh et al. 1999), the disruption of various E-cadherin-dependent functions by EC4 and EC5 hyper-glycosylation (Jamal et al. 2009; Pinho et al. 2011; Zhao et al. 2008a), or inhibition of E-cadherin adhesion by the DECMA-1 blocking antibody (Ozawa et al. 1990). The conundrum is due in part to the current absence of structural evidence for EC3-5 interactions, despite experimental evidence that this region affects adhesion. At the same time, the *cis* interface proposed on the basis of structures (Harrison et al. 2011; Wu et al. 2010) has not been verified by other approaches (Haussinger et al. 2002; Pokutta et al. 1994; Sivasankar et al. 2009). Further studies are needed to resolve these findings.

Third, physical chemical differences between molecular interactions in solution (3D) versus inter-membrane gaps (2D) also likely affect experimental outcomes. The effect of molecular confinement on protein folding is well known (Cheung et al. 2005; Cheung and Thirumalai 2007; Dhar et al. 2010), but the impact on protein functions at cell–cell junctions is only recently attracting attention. Functionally significant differences between 3D and 2D affinities are not explained solely by simple geometric corrections. Molecular length, cell topology, clustering, and lateral diffusivity also affect 2D affinities (Chen et al. 2008; Huang et al. 2004; Williams et al. 2001). Computer simulations suggest that molecular confinement could facilitate weak lateral cadherin interactions. Although this could enhance the putative *cis* interaction seen in structures (Wu et al. 2011), it could also promote other EC domain interactions for which biophysical evidence exists. For example, the two-stage kinetic signature (Fig. 4.3g), which may involve *cis* interactions, requires EC3-5 (Chien et al. 2008). As yet, there is no comprehensive, experimentally testable theoretical model for cadherin binding. Consequently, there is currently no method for testing models that might reconcile apparent differences between experimentally measured adhesion and solution binding data.

So far, a complete picture has yet to emerge that reconciles all of the available structural and functional data. However, new structures, additional biophysical studies, and now computer simulations continue to generate new insights into cadherin binding mechanisms. Some differences have yet to be resolved, but recent

results demonstrate the increasing consistencies between experimental findings and highlight physical chemical bases for experimental outcomes.

Acknowledgments DEL was supported by NSF CBET 0853705 and by NIH R21 HD059002. SS was supported by the Basil O'Connor Starter Scholar Award from the March of Dimes Foundation (#5-FY10-51).

References

Baumgartner W, Hinterdorfer P, Ness W, Raab A, Vestweber D, Schindler H, Drenckhahn D (2000) Cadherin interaction probed by atomic force microscopy. Proc Natl Acad Sci USA 97:4005–4010

Bayas MV, Leung A, Evans E, Leckband D (2006) Lifetime measurements reveal kinetic differences between homophilic cadherin bonds. Biophys J 90:1385–1395

Bayas MV, Kearney A, Avramovic A, van der Merwe PA, Leckband DE (2007) Impact of salt bridges on the equilibrium binding and adhesion of human CD2 and CD58. J Biol Chem 282:5589–5596

Becker KF, Kremmer E, Eulitz M, Becker I, Handschuh G, Schuhmacher C, Muller W, Gabbert HE, Ochiai A, Hirohashi S, Hofler H (1999) Analysis of E-cadherin in diffuse-type gastric cancer using a mutation-specific monoclonal antibody. Am J Pathol 155:1803–1809

Berx G, Nollet F, van Roy F (1998) Dysregulation of the E-cadherin/catenin complex by irreversible mutations in human carcinomas. Cell Adhes Commun 6:171–184

Bibert S, Jaquinod M, Concord E, Ebel C, Hewat E, Vanbelle C, Legrand P, Weidenhaupt M, Vernet T, Gulino-Debrac D (2002) Synergy between extracellular modules of vascular endothelial cadherin promotes homotypic hexameric interactions. J Biol Chem 277:12790–12801

Bixby JL, Zhang R (1990) Purified N-cadherin is a potent substrate for the rapid induction of neurite outgrowth. J Cell Biol 110:1253–1260

Boggon TJ, Eck MJ (2004) Structure and regulation of Src family kinases. Oncogene 23:7918–7927

Boggon TJ, Murray J, Chappuis-Flament S, Wong E, Gumbiner BM, Shapiro L (2002) C-cadherin ectodomain structure and implications for cell adhesion mechanisms. Science 296:1308–1313

Brasch J, Harrison OJ, Ahlsen G, Carnally SM, Henderson RM, Honig B, Shapiro L (2011) Structure and binding mechanism of vascular endothelial cadherin: a divergent classical cadherin. J Mol Biol 408:57–73

Brieher WM, Yap AS, Gumbiner BM (1996) Lateral dimerization is required for the homophilic binding activity of C-cadherin. J Cell Biol 135:487–496

Chappuis-Flament S, Wong E, Hicks LD, Kay CM, Gumbiner BM (2001) Multiple cadherin extracellular repeats mediate homophilic binding and adhesion. J Cell Biol 154:231–243

Chen W, Zarnitsyna VI, Sarangapani KK, Huang J, Zhu C (2008) Measuring receptor-ligand binding kinetics on cell surfaces: from adhesion frequency to thermal fluctuation methods. Cell Mol Bioeng 1:276–288

Chesla SE, Selvaraj P, Zhu C (1998) Measuring two-dimensional receptor-ligand binding kinetics by micropipette. Biophys J 75:1553–1572

Chesla SE, Li P, Nagarajan S, Selvaraj P, Zhu C (2000) The membrane anchor influences ligand binding two-dimensional kinetic rates and three-dimensional affinity of FcgammaRIII (CD16). J Biol Chem 275:10235–10246

Cheung MS, Thirumalai D (2007) Effects of crowding and confinement on the structures of the transition state ensemble in proteins. J Phys Chem B 111:8250–8257

Cheung MS, Klimov D, Thirumalai D (2005) Molecular crowding enhances native state stability and refolding rates of globular proteins. Proc Natl Acad Sci USA 102:4753–4758

Chien YH, Jiang N, Li F, Zhang F, Zhu C, Leckband D (2008) Two stage cadherin kinetics require multiple extracellular domains but not the cytoplasmic region. J Biol Chem 283:1848–1856
Chtcheglova, LA, Wildling L, Waschke J, Drenckhahn D, Hinterdorfer P (2010) AFM functional imaging on vascular endothelial cells. J Mol Recogn 23:589–596
Ciatto C, Bahna F, Zampieri N, VanSteenhouse HC, Katsamba PS, Ahlsen G, Harrison OJ, Brasch J, Jin X, Posy S, Vendome J, Ranscht B, Jessell TM, Honig B, Shapiro L (2010) T-cadherin structures reveal a novel adhesive binding mechanism. Nat Struct Mol Biol 17:339–347
Dhar A, Samiotakis A, Ebbinghaus S, Nienhaus L, Homouz D, Gruebele M, Cheung MS (2010) Structure, function, and folding of phosphoglycerate kinase are strongly perturbed by macromolecular crowding. Proc Natl Acad Sci USA 107:17586–17591
Dudko OK (2009) Single-molecule mechanics: new insights from the escape-over-a-barrier problem. Proc Natl Acad Sci USA 106:8795–8796
Dudko OK, Hummer G, Szabo A (2006) Intrinsic rates and activation free energies from single-molecule pulling experiments. Phys Rev Lett 96:108101
Dudko OK, Mathe J, Szabo A, Meller A, Hummer G (2007) Extracting kinetics from single-molecule force spectroscopy: nanopore unzipping of DNA hairpins. Biophys J 92:4188–4195
Dudko OK, Hummer G, Szabo A (2008) Theory, analysis, and interpretation of single-molecule force spectroscopy experiments. Proc Natl Acad Sci USA 105:15755–15760
du Roure O, Buguin A, Feracci H, Silberzan P (2006) Homophilic interactions between cadherin fragments at the single molecule level: an AFM study. Langmuir 22:4680–4684
Evans E (1998) Energy landscapes of biomolecular adhesion and receptor anchoring at interfaces explored with dynamic force spectroscopy. Faraday Discuss:1–16
Evans E (2001) Probing the relation between force—lifetime—and chemistry in single molecular bonds. Ann Rev Biophys Biomol Struct 30:105–128
Evans E, Ritchie K (1997) Dynamic strength of molecular adhesion bonds. Biophys J 72:1541–1555
Evans EA, Calderwood DA (2007) Forces and bond dynamics in cell adhesion. Science 316:1148–1153
Fuchs M, Hutzler P, Handschuh G, Hermannstadter C, Brunner I, Hofler H, Luber B (2004) Dynamics of cell adhesion and motility in living cells is altered by a single amino acid change in E-cadherin fused to enhanced green fluorescent protein. Cell Motil Cytoskeleton 59:50–61
Gavard J, Lambert M, Grosheva I, Marthiens V, Irinopoulou T, Riou JF, Bershadsky A, Mege RM (2004) Lamellipodium extension and cadherin adhesion: two cell responses to cadherin activation relying on distinct signalling pathways. J Cell Sci 117:257–270
Geng F, Shi BZ, Yuan YF, Wu XZ (2004) The expression of core fucosylated E-cadherin in cancer cells and lung cancer patients: prognostic implications. Cell Res 14:423–433
Guo HB, Johnson H, Randolph M, Pierce M (2009) Regulation of homotypic cell-cell adhesion by branched N-glycosylation of N-cadherin extracellular EC2 and EC3 domains. J Biol Chem 284:34986–34997
Handschuh G, Candidus S, Luber B, Reich U, Schott C, Oswald S, Becke H, Hutzler P, Birchmeier W, Hofler H, Becker KF (1999) Tumour-associated E-cadherin mutations alter cellular morphology, decrease cellular adhesion and increase cellular motility. Oncogene 18:4301–4312
Handschuh G, Luber B, Hutzler P, Hofler H, Becker KF (2001) Single amino acid substitutions in conserved extracellular domains of E-cadherin differ in their functional consequences. J Mol Biol 314:445–454
Harrison OJ, Corps EM, Berge T, Kilshaw PJ (2005) The mechanism of cell adhesion by classical cadherins: the role of domain 1. J Cell Sci 118:711–721
Harrison OJ, Bahna F, Katsamba PS, Jin X, Brasch J, Vendome J, Ahlsen G, Carroll KJ, Price SR, Honig B, Shapiro L (2010) Two-step adhesive binding by classical cadherins. Nat Struct Mol Biol 17:348–357
Harrison OJ, Jin X, Hong S, Bahna F, Ahlsen G, Brasch J, Wu Y, Vendome J, Felsovalyi K, Hampton CM, Troyanovsky RB, Ben-Shaul A, Frank J, Troyanovsky SM, Shapiro L, Honig B (2011) The extracellular architecture of adherens junctions revealed by crystal structures of type I cadherins. Structure 19:244–256

Haussinger D, Ahrens T, Sass HJ, Pertz O, Engel J, Grzesiek S (2002) Calcium-dependent homoassociation of E-cadherin by NMR spectroscopy: changes in mobility, conformation and mapping of contact regions. J Mol Biol 324:823–839

Haussinger D, Ahrens T, Aberle T, Engel J, Stetefeld J, Grzesiek S (2004) Proteolytic E-cadherin activation followed by solution NMR and X-ray crystallography. EMBO J 23:1699–1708

He W, Cowin P, Stokes DL (2003) Untangling desmosomal knots with electron tomography. Science 302:109–113

Hewat EA, Durmort C, Jacquamet L, Concord E, Gulino-Debrac D (2007) Architecture of the VE-cadherin hexamer. J Mol Biol 365:744–751

Homola J (2008) Surface plasmon resonance sensors for detection of chemical and biological species. Chem Rev 108:462–493

Hong S, Troyanovsky RB, Troyanovsky SM (2011) Cadherin exits the junction by switching its adhesive bond. J Cell Biol 192:1073–1083

Huang J, Chen J, Chesla SE, Yago T, Mehta P, McEver RP, Zhu C, Long M (2004) Quantifying the effects of molecular orientation and length on two-dimensional receptor-ligand binding kinetics. J Biol Chem 279:44915–44923

Huang J, Edwards LJ, Evavold BD, Zhu C (2007) Kinetics of MHC-CD8 interaction at the T cell membrane. J Immunol 179:7653–7662

Huang J, Zarnitsyna VI, Liu B, Edwards LJ, Jiang N, Evavold BD, Zhu C (2010) The kinetics of two-dimensional TCR and pMHC interactions determine T-cell responsiveness. Nature 464:932–936

Iino R, Koyama I, Kusumi A (2001) Single molecule imaging of green fluorescent proteins in living cells: E-cadherin forms oligomers on the free cell surface. Biophys J 80:2667–2677

Israelachvili J (1992) Adhesion forces between surfaces in liquids and condensable vapours. Surface Sci Rep 14:110–159

Israelachvili JN, Adams GE (1978) Measurement of forces between two mica surfaces in aqueous electrolyte solutions in the range 0–100 nm. J Chem Soc Faraday Trans I 75:975–1001

Jamal BT, Nita-Lazar M, Gao Z, Amin B, Walker J, Kukuruzinska MA (2009) N-glycosylation status of E-cadherin controls cytoskeletal dynamics through the organization of distinct beta-catenin- and gamma-catenin-containing AJs. Cell Health Cytoskelet 2009:67–80

Johnson CP, Fujimoto I, Perrin-Tricaud C, Rutishauser U, Leckband D (2004) Mechanism of homophilic adhesion by the neural cell adhesion molecule: use of multiple domains and flexibility. Proc Natl Acad Sci USA 101:6963–6968

Johnson CP, Fragneto G, Konovalov O, Dubosclard V, Legrand JF, Leckband DE (2005a) Structural studies of the neural-cell-adhesion molecule by X-ray and neutron reflectivity. Biochemistry 44:546–554

Johnson CP, Fujimoto I, Rutishauser U, Leckband DE (2005b) Direct evidence that neural cell adhesion molecule (NCAM) polysialylation increases intermembrane repulsion and abrogates adhesion. J Biol Chem 280:137–145

Katsamba P, Carroll K, Ahlsen G, Bahna F, Vendome J, Posy S, Rajebhosale M, Price S, Jessell TM, Ben-Shaul A, Shapiro L, Honig BH (2009) Linking molecular affinity and cellular specificity in cadherin-mediated adhesion. Proc Natl Acad Sci USA 106:11594–11599

Kim YJ, Johnson KR, Wheelock MJ (2005) N-cadherin-mediated cell motility requires cis dimers. Cell Commun Adhes 12:23–39

Kitagawa M, Natori M, Murase S, Hirano S, Taketani S, Suzuki ST (2000) Mutation analysis of cadherin-4 reveals amino acid residues of EC1 important for the structure and function. Biochem Biophys Res Commun 271:358–363

Klingelhofer J, Laur OY, Troyanovsky RB, Troyanovsky SM (2002) Dynamic interplay between adhesive and lateral E-cadherin dimers. Mol Cell Biol 22:7449–7458

Koch AW, Pokutta S, Lustig A, Engel J (1997) Calcium binding and homoassociation of E-cadherin domains. Biochemistry 36:7697–7705

Koch AW, Bozic D, Pertz O, Engel J (1999) Homophilic adhesion by cadherins. Curr Opin Struct Biol 9:275–281

Lambert O, Taveau JC, Him JL, Al Kurdi R, Gulino-Debrac D, Brisson A (2005) The basic framework of VE-cadherin junctions revealed by cryo-EM. J Mol Biol 346:1193–1196
Lebowitz J, Lewis MS, Schuck P (2002) Modern analytical ultracentrifugation in protein science: a tutorial review. Protein Sci 11:2067–2079
Leckband D (2000) Measuring the forces that control protein interactions. Annu Rev Biophys Biomol Struct 29:1–26
Leckband D, Israelachvili J (2001) Intermolecular forces in biology. Q Rev Biophys 34:105–267
Leckband D, Prakasam A (2006) Mechanism and dynamics of cadherin adhesion. Annu Rev Biomed Eng 8:259–287
Leckband D, Sivasankar S (2000) Mechanism of homophilic cadherin adhesion. Curr Opin Cell Biol 12:587–592
Leckband DE, Schmitt FJ, Israelachvili JN, Knoll W (1994) Direct force measurements of specific and nonspecific protein interactions. Biochemistry 33:4611–4624
Leckband D, Muller W, Schmitt FJ, Ringsdorf H (1995a) Molecular mechanisms determining the strength of receptor-mediated intermembrane adhesion. Biophys J. 69:1162–1169
Leckband DE, Kuhl T, Wang HK, Herron J, Muller W, Ringsdorf H (1995b). 4-4-20 anti-fluorescyl IgG Fab' recognition of membrane bound hapten: direct evidence for the role of protein and interfacial structure. Biochemistry 34:11467–11478
Leckband DE, Menon S, Rosenberg K, Graham SA, Taylor ME, Drickamer K (2011) Geometry and adhesion of extracellular domains of DC-SIGNR neck length variants analyzed by force-distance measurements. Biochemistry 50:6125–6132
Liwosz A, Lei T, Kukuruzinska MA (2006) N-glycosylation affects the molecular organization and stability of E-cadherin junctions. J Biol Chem 281:23138–23149
Long M, Zhao H, Huang KS, Zhu C (2001) Kinetic measurements of cell surface E-selectin/carbohydrate ligand interactions. Annals Biomed Eng 29:935–946
Luber B, Candidus S, Handschuh G, Mentele E, Hutzler P, Feller S, Voss J, Hofler H, Becker KF (2000) Tumor-derived mutated E-cadherin influences beta-catenin localization and increases susceptibility to actin cytoskeletal changes induced by pervanadate. Cell Adhes Commun. 7:391–408
Marshall BT, Long M, Piper JW, Yago T, McEver RP, Zhu C (2003) Direct observation of catch bonds involving cell-adhesion molecules. Nature 423:190–193
Menon S, Rosenberg K, Graham SA, Ward EM, Taylor ME, Drickamer K, Leckband DE (2009) Binding-site geometry and flexibility in DC-SIGN demonstrated with surface force measurements. Proc Natl Acad Sci USA 106:11524–11529
Miloushev VZ, Bahna F, Ciatto C, Ahlsen G, Honig B, Shapiro L, Palmer AG 3rd (2008) Dynamic properties of a type II cadherin adhesive domain: implications for the mechanism of strand-swapping of classical cadherins. Structure 16:1195–1205
Nagar B, Overduin M, Ikura M, Rini JM (1996) Structural basis of calcium-induced E-cadherin rigidification and dimerization. Nature 380:360–364
Nita-Lazar M, Rebustini I, Walker J, Kukuruzinska MA (2010) Hypoglycosylated E-cadherin promotes the assembly of tight junctions through the recruitment of PP2A to adherens junctions. Exp Cell Res 316:1871–1884
Nose A, Nagafuchi A, Takeichi M (1988) Expressed recombinant cadherins mediate cell sorting in model systems. Cell 54:993–1001
Nose A, Tsuji K, Takeichi M (1990) Localization of specificity determining sites in cadherin cell adhesion molecules. Cell 61:147–155
Ozawa M, Hoschutzky H, Herrenknecht K, Kemler R (1990) A possible new adhesive site in the cell-adhesion molecule uvomorulin. Mech Dev 33:49–56
Perret E, Leung A, Feracci H, Evans E (2004) Trans-bonded pairs of E-cadherin exhibit a remarkable hierarchy of mechanical strengths. Proc Natl Acad Sci USA 101:16472–16477
Pertsinidis A, Zhang Y, Chu S (2010) Subnanometre single-molecule localization, registration and distance measurements. Nature 466:647–651
Pertz O, Bozic D, Koch AW, Fauser C, Brancaccio A, Engel J (1999) A new crystal structure, Ca^{2+} dependence and mutational analysis reveal molecular details of E-cadherin homoassociation. EMBO J 18:1738–1747

Pinho SS, Osorio H, Nita-Lazar M, Gomes J, Lopes C, Gartner F, Reis CA (2009) Role of E-cadherin N-glycosylation profile in a mammary tumor model. Biochim Biophys Res Comm 379:1091–1096

Pinho SS, Seruca R, Gartner F, Yamaguchi Y, Gu J, Taniguchi N, Reis CA (2011) Modulation of E-cadherin function and dysfunction by N-glycosylation. Cell Mol Life Sci 68:1011–1020

Piper JW, Swerlick RA, Zhu C (1998) Determining force dependence of two-dimensional receptor-ligand binding affinity by centrifugation. Biophys J 74:492–513

Pokutta S, Herrenknecht K, Kemler R, Engel J (1994) Conformational changes of the recombinant extracellular domain of E-cadherin upon calcium binding. Eur J Biochem 223:1019–1026

Prakasam A, Chien YH, Maruthamuthu V, Leckband DE (2006a) Calcium site mutations in cadherin: impact on adhesion and evidence of cooperativity. Biochemistry 45:6930–6939

Prakasam AK, Maruthamuthu V, Leckband DE (2006b) Similarities between heterophilic and homophilic cadherin adhesion. Proc Natl Acad Sci USA 103:15434–15439

Prasad A, Pedigo S (2005) Calcium-dependent stability studies of domains 1 and 2 of epithelial cadherin. Biochemistry 44:13692–13701

Roy R, Hohng S, Ha T (2008) A practical guide to single-molecule FRET. Nature Methods 5:507–516

Scott JA, Shewan AM, den Elzen NR, Loureiro JJ, Gertler FB, Yap AS (2006) Ena/VASP proteins can regulate distinct modes of actin organization at cadherin-adhesive contacts. Mol Biol Cell. 17:1085–1095

Shan W, Yagita Y, Wang Z, Koch A, Fex Svenningsen A, Gruzglin E, Pedraza L, Colman DR (2004) The minimal essential unit for cadherin-mediated intercellular adhesion comprises extracellular domains 1 and 2. J Biol Chem 279:55914–55923

Shi Q, Chien YH, Leckband D (2008) Biophysical properties of cadherin bonds do not predict cell sorting. J Biol Chem 283:28454–28463

Shi Q, Maruthamuthu V, Leckband D (2010) Allosteric cross-talk between cadherin ectodomains. Biophys J 99:95–104

Sivasankar S, Subramaniam S, Leckband D (1998) Direct molecular level measurements of the electrostatic properties of a protein surface. Proc Natl Acad Sci USA 95:12961–12966

Sivasankar S, Gumbiner B, Leckband D (2001) Direct measurements of multiple adhesive alignments and unbinding trajectories between cadherin extracellular domains. Biophys J 80:1758–1768

Sivasankar S, Zhang Y, Nelson WJ, Chu S (2009) Characterizing the initial encounter complex in cadherin adhesion. Structure 17:1075–1081

Smutney M, Cox H, Leerberg J, Conti M, Ferguson C, Hamilton N, Parton R, Adeslstein R, Yap A (2010) Myosin II isoforms identify distinct functional modules that support integrity of the epithelial zonula adherens. Nat Cell Biol 12:696–702

Sotomayor M, Schulten K (2008) The allosteric role of the Ca^{2+} switch in adhesion and elasticity of C-cadherin. Biophys J 94:4621–4633

Suzuki Y, Dudko OK (2010) Single-molecule rupture dynamics on multidimensional landscapes. Phys Rev Lett 104:048101

Takeda H, Shimoyama Y, Nagafuchi A, Hirohashi S (1999) E-cadherin functions as a cis-dimer at the cell-cell adhesive interface in vivo. Nat Struct Biol 6:310–312

Tamura K, Shan WS, Hendrickson WA, Colman DR, Shapiro L (1998) Structure-function analysis of cell adhesion by neural (N-) cadherin. Neuron 20:1153–1163

Taveau JC, Dubois M, Le Bihan O, Trepout S, Almagro S, Hewat E, Durmort C, Heyraud S, Gulino-Debrac D, Lambert O (2008) Structure of artificial and natural VE-cadherin-based adherens junctions. Biochem Soc Trans 36:189–193

Thomas W (2008) Catch bonds in adhesion. Annu Rev Biomed Eng 10:39–57

Thomas WE (2009) Mechanochemistry of receptor-ligand bonds. Curr Opin Struct Biol 19:50–55

Tomschy A, Fauser C, Landwehr R, Engel J (1996) Homophilic adhesion of E-cadherin occurs by a co-operative two-step interaction of N-terminal domains. EMBO J 15:3507–3514

Troyanovsky RB, Sokolov E, Troyanovsky SM (2003) Adhesive and lateral E-cadherin dimers are mediated by the same interface. Mol Cell Biol 23:7965–7972

Tsukasaki Y, Kitamura K, Shimizu K, Iwane AH, Takai Y, Yanagida T (2007) Role of multiple bonds between the single cell adhesion molecules, nectin and cadherin, revealed by high sensitive force measurements. J Mol Biol 367:996–1006

Vendome J, Posy S, Jin X, Bahna F, Ahlsen G, Shapiro L, Honig B (2011) Molecular design principles underlying beta-strand swapping in the adhesive dimerization of cadherins. Nat Struct Mol Biol 18:693–700

Vunnam N, Pedigo S (2011a) Prolines in betaA-sheet of neural cadherin act as a switch to control the dynamics of the equilibrium between monomer and dimer. Biochemistry 50:6959–6965

Vunnam N, Pedigo S (2011b) Sequential binding of calcium leads to dimerization in neural cadherin. Biochemistry 50:2973–2982

Williams TE, Nagarajan S, Selvaraj P, Zhu C (2001) Quantifying the impact of membrane microtopology on effective two-dimensional affinity. J Biol Chem 276:13283–13288

Wu Y, Jin X, Harrison O, Shapiro L, Honig BH, Ben-Shaul A (2010) Cooperativity between trans and cis interactions in cadherin-mediated junction formation. Proc Natl Acad Sci USA 107:17592–17597

Wu Y, Vendome J, Shapiro L, Ben-Shaul A, Honig B (2011) Transforming binding affinities from three dimensions to two with application to cadherin clustering. Nature 475:510–513

Yeung C, Purves T, Kloss AA, Kuhl TL, Sligar S, Leckband D (1999) Cytochrome c recognition of immobilized, orientational variants of cytochrome b5: direct force and equilibrium binding measurements. Langmuir 15:6829–6836

Zhang F, Marcus WD, Goyal NH, Selvaraj P, Springer TA, Zhu C (2005) Two-dimensional kinetics regulation of alphaLbeta2-ICAM-1 interaction by conformational changes of the alphaL-inserted domain. J Biol Chem 280:42207–42218

Zhang Y, Sivasankar S, Nelson WJ, Chu S (2009) Resolving cadherin interactions and binding cooperativity at the single-molecule level. Proc Natl Acad Sci USA 106:109–114

Zhao H, Liang Y, Xu Z, Wang L, Zhou F, Li Z, Jin J, Yang Y, Fang Z, Hu Y, Zhang L, Su J, Zha X (2008a) N-glycosylation affects the adhesive function of E-Cadherin through modifying the composition of adherens junctions (AJs) in human breast carcinoma cell line MDA-MB-435. J Cell Biochem 104:162–175

Zhao Y, Sato Y, Isaji T, Fukuda T, Matsumoto A, Miyoshi E, Gu J, Taniguchi N (2008b) Branched N-glycans regulate the biological functions of integrins and cadherins. Febs J 275:1939–1948

Zhong Y, Brieher WM, Gumbiner BM (1999) Analysis of C-cadherin regulation during tissue morphogenesis with an activating antibody. J Cell Biol 144:351–359

Zhu B, Davies EA, van der Merwe PA, Calvert T, Leckband DE (2002) Direct measurements of heterotypic adhesion between the cell surface proteins CD2 and CD48. Biochemistry 41:12163–12170

Zhu B, Chappuis-Flament S, Wong E, Jensen IE, Gumbiner BM, Leckband D (2003) Functional analysis of the structural basis of homophilic cadherin adhesion. Biophys J 84:4033–4042

Zhu C, Yago T, Lou J, Zarnitsyna VI, McEver RP (2008) Mechanisms for flow-enhanced cell adhesion. Ann Biomed Eng 36:604–621